

Assessment of cerebral iron content in patients with Parkinson's disease by the susceptibility-weighted MRI

S.-F. WU, Z.-F. ZHU, Y. KONG, H.-P. ZHANG, G.-Q. ZHOU, Q.-T. JIANG, X.-P. MENG

Department of Neurology, Affiliated Jiangyin Hospital Medical College of Southeast University, Jiangyin Jiangsu Province, China

Abstract. – OBJECTIVE: The overall goal of this study was to evaluate the usability of the susceptibility weighted imaging (SWI) in (1) assessment of iron deposition to enhance our ability to detect PD in the early phase and (2) in estimation of the degree of PD.

PATIENTS AND METHODS: SWI scans were carried out in 54 patients with PD (18 patients with the Hoehn-Yahr scale < 1.5 and 36 patients with the Hoehn-Yahr stage > 1.5) and 40 control individuals. The phase values of the substantia nigra, red nucleus, caudate nucleus, putamen, and globus pallidus were measured on the corrected phase image.

RESULTS: Compared with control individuals, patients with both the early and intermediate/advanced stages of PD had significantly different phase values in the substantia nigra, red nucleus, caudate nucleus, putamen, and globus pallidus (all $p < 0.05$). The phase values of the substantia nigra and globus pallidus inversely correlated with the Hoehn-Yahr scale (respectively, $r = -0.845$, $p < 0.05$, and $r = -0.868$, $p < 0.05$). Weaker correlations were found between the phase values of red nucleus, caudate nucleus, putamen, and Hoehn-Yahr scale (red nucleus $r = -0.543$, caudate nucleus $r = -0.620$, $p < 0.05$, putamen $r = -0.537$).

CONCLUSIONS: A semi-quantitative assessment of the iron content of the substantia nigra and globus pallidus with the help of SWI may be useful for early diagnosis of PD and evaluation of the degree of this disease.

Key words:

Parkinson's disease, Susceptibility weighted imaging, Cerebellar gray nucleus, Iron deposition.

Introduction

Parkinson's disease (PD) is a neurodegenerative disease commonly seen in elderly individuals. It is estimated that 1% of people over 60 years old have PD¹. The pathogenetic mechanism of PD comprises degeneration of dopaminergic neurons. The Lewy body formation induces a ni-

grostriatal pathway damage and reduction of dopamine levels in the caudate nucleus and putamen. An abnormal iron metabolism is thought to play a role in the pathogenesis².

The Susceptibility-Weighted Imaging (SWI) utilizes magnetic susceptibility differences and uses pulse sequences to enhance the contrast. SWI is capable of showing non-heme iron (e.g., ferritin) clearer than other techniques³. In the present study, we utilized the 3.0T ultra-high field strength SWI to semi-quantitatively assess iron deposition in the cerebral nuclei of patients with PD by measuring the phase value from the corrected phase image. The overall goal was to evaluate the usability of SWI in (1) assessment of iron deposition to enhance our ability to detect PD in the early phase and (2) in estimation of the degree of PD.

Patients and Methods

Patients

The data were collected from 54 patients with PD who were treated in our Hospital from January 2012 to December 2012. There were 33 male and 21 female patients whose mean (\pm SD) age was 65.6 ± 5.8 years. The diagnosis of PD was made by two neurologists in line with the United Kingdom Parkinson's Disease Society Brain Clinical Diagnostic Criteria⁴. Patients with encephalitis, cerebral vascular disease, poisoning, drug-induced Parkinsonism, and Parkinson's plus syndrome were excluded. The patients were stratified according to their severity grading by the Hoehn-Yahr scale⁵: early PD (Hoehn-Yahr scale of < 1.5; 18 patients) and intermediate/advanced PD (Hoehn-Yahr scale ≥ 1.5 ; 36 patients). Forty healthy individuals were chosen as controls whose age and gender distribution matched those of patients with PD. There were 18 female and 22 male healthy individuals with a mean age of 66.5 ± 6.0 years.

Instruments

The Philips 3.0T superconductive MRI system (Philips, Amsterdam, The Netherlands) was used. Study individuals were asked to lie on their backs and tested using an eight-channel phased array coil fixed to the head and neck. The patient's head was positioned in the midline between both shoulders. Cushions were used to help to maintain the head position. Horizontal and sagittal T1WI, T2WI, and SWI scans were carried out in all patients. The MR data acquisition sequences and parameters were as follows: cross sectional spin-echo (SE) sequences, axial and sagittal T1WI sequence (TR 600 ms, TE 15 ms), axial T2WI sequence (TR 3600 ms, TE 90 ms) and FLAIR sequences (TR 10000 ms, TE 115 ms), slice thickness 5.5 mm, slice spacing 1.2 mm, FOV 24 × 24 cm, matrix size 384 × 512. The MR scanning position of each axis was kept consistent. SWI used 3D gradient-echo sequence whose parameters were set as follows: TR 33.0 ms, TE 20.0 ms, flip angle 15°, bandwidth 48.00 Hz, slice thickness 1.5 mm, slice spacing 0, matrix size 448 × 384.

Image processing and analysis

Post image processing was performed on Philips Workstation after data acquisition with SWI scan. All images were read by two experienced radiologists who excluded cerebral lesions manually marked the region of interest, and measured phase values of caudate nucleus head, putamen, globus pallidus, substantia nigra, red nucleus, which are the areas of iron deposition. The radiologists were blinded to the individuals' grouping. The phase values were presented in forms of mean ± SD in term of radian. We specifically avoided regions with calcification and visible lesions. The corrected phase image was obtained and combined with the magnitude data with weighting to produce final SWI images. Two sides from the same region were evaluated, and for each

side a triplicate measurement was performed to obtain mean value to reduce potential bias. The same scanning plane was chosen for all subjects. The measurement methods and data processing methods were as per Philips recommendations.

Statistical Analysis

The SPSS17.0 statistical software package (SPSS Statistics, IBM, USA) was used. Data are presented as mean ± SD. The phase values of patients with PD were compared with control values: the *t* test was used for data that were normally distributed, while the non-parametric Mann-Whitney U test was utilized for not normally distributed data. The Spearman correlation analysis was utilized to evaluate correlation between phase values and Hoehn-Yahr scale of each PD subgroup, and coefficients were compared by *t* test. $p < 0.05$ was considered statistically significant.

Results

We first compared data from control individuals and early PD. The corrected phase image had a higher resolution compared with conventional scanning. Therefore, the region of interest (ROI) was set at the low signal iron deposition zone, and phase values were measured. The two-way *t*-test was applied to compare phase values of each brain region (Table I). There were significant differences in phase values of caudate nucleus head, putamen, globus pallidus, substantia nigra, and red nucleus between control individuals and patients with early PD (all $p < 0.05$). Figure 1 shows SWI phase values of substantia nigra of control individuals and patients with early PD.

Then, we compared parameters between control individuals and patients with intermediate/ advanced PD. On a corrected phase image, ROI was set at low signal iron deposition region, and phase

Table I. Comparison of corrected phase values between groups.

Grey matter nuclei	Control group	Early stage PD	p^a	Intermediate and advanced PD	p^b
Substantia nigra	-0.101 ± 0.019	-0.125 ± 0.016	0.005	-0.131 ± 0.013	0.002
Red nucleus	-0.092 ± 0.020	-0.091 ± 0.025	0.043	-0.106 ± 0.017	0.023
Caudate nucleus	-0.061 ± 0.009	-0.065 ± 0.013	0.012	-0.072 ± 0.015	0.010
Putamen	-0.071 ± 0.021	-0.073 ± 0.019	0.023	-0.075 ± 0.021	0.013
Globus pallidus	-0.076 ± 0.014	-0.082 ± 0.018	0.002	-0.093 ± 0.031	0.001

Footnote: Data are presented as control (mean ± SD). p^a = early stage PD vs. control group; p^b = intermediate and advanced PD vs. control group.

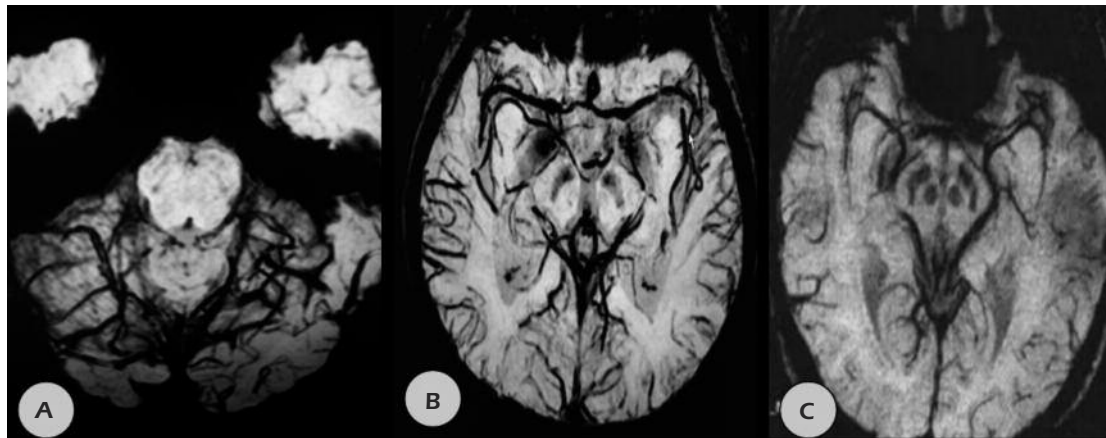


Figure 1. SWI phase values of substantia nigra of (A) control group (-0.901), (B) early PD group (0.110), and (C) intermediate/advanced PD group (0.130).

values were measured again (Table I). As before, all values were significantly (all $p < 0.05$) different in patients with intermediate and advanced PD.

Correlations between Hoehn-Yahr scale and phase values were quantified in both PD groups. Patients with early PD (Hoehn-Yahr scale < 1.5) included 9 patients with stage 1 and 9 with stage 1.5, while the intermediate/advanced PD group (Hoehn-Yahr scale ≥ 1.5) included 7 patients with stage 2, 8 with stage 2.5, 7 with stage 3, 8 with stage 4, and 6 with stage 5. The correlation analysis demonstrated that phase values significantly and inversely correlated with the Hoehn-Yahr scale in caudate nucleus head and globus pallidus (respectively, $r = -0.845$, $p = 0.021$, and $r = -0.868$, $p = 0.024$). This correlation was weaker in red nucleus, putamen and substantia nigra (respectively, $r = -0.543$, $p = 0.013$, $r = -0.537$, $p = 0.023$, $r = -0.620$, $p = 0.032$).

Discussion

Neuropathological basis of PD is the degeneration of dopaminergic neurons in substantia nigra and subsequent reduction of dopamine level in corpus striatum. The exact mechanism of iron involvement in PD is unclear. Iron metabolism is a complex process that includes iron uptake, storage and transport, and involves many proteins, such as transferrin, transferrin receptor, ferritin, copper-protein, and others⁶. In PD, iron levels increase without a corresponding rise in ferritin levels, which leads to an enhanced level of free iron in the brain. There is currently no unified theory to explain this phenomenon. Most researchers believe that this is relat-

ed to abnormal expression of ferritin^{7,8}. Iron deposition increases gradually in the nervous system along with the progression of the disease, which is especially true for the basal ganglia. The main toxicological effect of iron deposition originates from highly cytotoxic hydroxyl radicals which are the products of Fenton reaction. Hydroxyl radicals can cause damages to proteins, nucleic acids and cell membranes, with the latter comprising high levels of unsaturated fatty acids. Accumulation of hydroxyl radicals can eventually lead to cell death.

SWI can show magnetic susceptibility differences between ferrous and non-ferrous tissues. It also can be used to measure iron content changes in local brain regions^{9,10}. In specific, when the phase image is corrected after the filtering process, SWI can show the changes in the phase of proton spin caused by uneven local magnetic field due to the presence of magnetic material. High levels of iron in red nucleus and substantia nigra cause changes in magnetic susceptibility and a decrease in the phase value. Calcium is a typical diamagnetic substance and calcification is mainly shown as high signal in the phase diagram¹¹.

Our study demonstrates that patients with PD have various degrees of iron deposition in the basal ganglia and that iron deposition increases along with progression of the disease. However, our observations are different from a previous study¹² which showed that iron deposition levels in the globus pallidus and putamen are lower in PD if evaluated by the T2-weighted imaging. We believe that our findings are more reliable because SWI is more sensitive to iron than T2-weighted imaging. Further, Graham et al¹³ used 1.5T MR and SWI imaging and also demon-

strated increased iron deposition level in substantia nigra which is in agreement with our study. However, using the susceptibility weighted MRI, Huang et al¹⁴ found that iron levels in the substantia nigra and globus pallidus were significantly different between patients with PD and healthy individuals, while there was no difference in iron levels in the red nucleus, caudate nucleus head, and putamen. The discrepancy between our and their findings may be a result of different sampling size and different inclusion criteria.

In our study, phase values of each region of basal ganglia were found to significantly and inversely correlate to the degree of PD. The phase values of substantia nigra and globus pallidus were in a better agreement with the Hoehn-Yahr scale than the values for other tested regions. However, Shen et al¹⁵ only found such negative correlation in substantia nigra and globus pallidus. This discrepancy may also be a result of differences in the sampling size and inclusion criteria.

Conclusions

Assessment of basal ganglia phase values and semi-quantitative evaluation of iron deposition content in patients with PD using SWI imaging may help to obtain insights into early pathological changes, which would be beneficial for earlier diagnosis. This technique also provides reliable imaging data and enriches the information available for further clinical examination or treatments. Due to constant advances in the MRI technology, especially in the 3.0T MRI with its high signal-to-noise ratio, high chemical shift and high magnetic susceptibility effects also evolves. Studies of iron deposition in patients with PD using SWI imaging definitely can facilitate early diagnosis, better treatment stratification, and a more accurate prognosis.

Conflict of Interest

The Authors declare that there are no conflicts of interest.

References

- 1) DE LAU LM, BRETELER MM. Epidemiology of Parkinson's disease. *Lancet Neurol* 2006; 5: 525-535.
- 2) OAKLEY AE, COLLINGWOOD JF, DOBSON J, LOVE G, PERROTT HR, EDWARDS JA, ELSTNER M, MORRIS CM. Individual dopaminergic neurons show raised iron levels in Parkinson disease. *Neurology* 2007; 68: 1820-1825.
- 3) THOMAS B, SOMASUNDARAM S, THAMBURAJ K, KESAVADAS C, GUPTA AK, BODHEY NK, KAPILAMOORTHY TR. Clinical applications of susceptibility weighted MR imaging of the brain--a pictorial review. *Neuroradiology* 2008; 50: 105-116.
- 4) HUGHES AJ, DANIEL SE, KILFORD L, LEES AJ. Accuracy of clinical diagnosis of idiopathic Parkinson's disease: a clinico-pathological study of 100 cases. *J Neurol Neurosurg Psychiatry* 1992; 55: 181-184.
- 5) HOEHN MM, YAHR MD. Parkinsonism: onset, progression, and mortality. 1967. *Neurology* 2001; 57: S11-26.
- 6) MOOS T, ROSENGREN NIELSEN T, SKJORRINGE T, MORGAN EH. Iron trafficking inside the brain. *J Neurochem* 2007; 103: 1730-1740.
- 7) BERG D. Disturbance of iron metabolism as a contributing factor to SN hyperechogenicity in Parkinson's disease: implications for idiopathic and monogenetic forms. *Neurochem Res* 2007; 32: 1646-1654.
- 8) KANO O, IKEDA K, IWASAKI Y, JIANG H. Decreased iron levels in the temporal cortex in postmortem human brains with Parkinson disease. *Neurology* 2013; 81: 1181-1182.
- 9) ROSSI M, RUOTTINEN H, ELOVAARA I, RYMIN P, SOIMAKALLIO S, ESKOLA H, DASTIDAR P. Brain iron deposition and sequence characteristics in Parkinsonism: comparison of SWI, T(2)* maps, T(2)-weighted-, and FLAIR-SPACE. *Invest Radiol* 2010; 45: 795-802.
- 10) KIRSCH W, McAULEY G, HOLSHOUSER B, PETERSEN F, AYAZ M, VINTERS HV, DICKSON C, HAACKE EM, BRITT W, 3RD, LARSEN J, KIM I, MUELLER C, SCHRAG M, KIDO D. Serial susceptibility weighted MRI measures brain iron and microbleeds in dementia. *J Alzheimers Dis* 2009; 17: 599-609.
- 11) FENG F, YOU H, HU L. [Preliminary study of susceptibility-weighted imaging in differentiation of multiple system atrophy and idiopathic Parkinson disease]. *Chin J Med Imaging Technol* 2007; 23: 781-784. in Chinese.
- 12) KOSTA P, ARGYROPOULOU MI, MARKOULA S, KONITSIOTIS S. MRI evaluation of the basal ganglia size and iron content in patients with Parkinson's disease. *J Neurol* 2006; 253: 26-32.
- 13) GRAHAM JM, PALEY MN, GRUNEWALD RA, HOGGARD N, GRIFFITHS PD. Brain iron deposition in Parkinson's disease imaged using the PRIME magnetic resonance sequence. *Brain* 2000; 123 Pt 12: 2423-2431.
- 14) HUANG XM, SUN B, XUE YJ, DUAN Q. [Susceptibility-weighted imaging in detecting brain iron accumulation of Parkinson's disease]. *Zhonghua Yi Xue Za Zhi* 2010; 90: 3054-3058. in Chinese.
- 15) SHEN X, CUI GY. [Application of measurement of brain iron content in patients with Parkinson's disease using susceptibility weighted MRI]. *Chin J Geriatr* 2010; 29: 980-983. in Chinese.